Available online at www.sciencedirect.com

ScienceDirect

Current Opinion in Chemical Biology

Stereo-electronic control of reaction selectivity in short-chain dehydrogenases: Decarboxylation, epimerization, and dehydration

Annika J. E. Borg[1], Koen Beerens[2], Martin Pfeiffer[1,3], Tom Desmet[2,3] and Bernd Nidetzky[1,3]

Abstract

Sugar nucleotide–modifying enzymes of the short-chain dehydrogenase/reductase type use transient oxidation–reduction by a tightly bound nicotinamide cofactor as a common strategy of catalysis to promote a diverse set of reactions, including decarboxylation, single- or double-site epimerization, and dehydration. Although the basic mechanistic principles have been worked out decades ago, the finely tuned control of reactivity and selectivity in several of these enzymes remains enigmatic. Recent evidence on uridine 5'-diphosphate (UDP)-glucuronic acid decarboxylases (UDP-xylose synthase, UDP-apiose/UDP-xylose synthase) and UDP-glucuronic acid-4-epimerase suggests that stereo-electronic constraints established at the enzyme's active site control the selectivity, and the timing of the catalytic reaction steps, in the conversion of the common substrate toward different products. The mechanistic idea of stereo-electronic control is extended to epimerases and dehydratases that deprotonate the Cα of the transient keto-hexose intermediate. The human guanosine 5'-diphosphate (GDP)-mannose 4,6-dehydratase was recently shown to use a minimal catalytic machinery, exactly as predicted earlier from theoretical considerations, for the β-elimination of water from the keto-hexose species.

Addresses

[1] Institute of Biotechnology and Biochemical Engineering, Graz University of Technology, NAWI Graz, 8010, Graz, Austria
[2] Centre for Synthetic Biology, Department of Biotechnology, Ghent University, 9000, Ghent, Belgium
[3] Austrian Centre of Industrial Biotechnology (acib), 8010, Graz, Austria

Corresponding author: Nidetzky, Bernd (bernd.nidetzky@tugraz.at)

Current Opinion in Chemical Biology 2021, **61**:43–52

This review comes from a themed issue on **Biocatalysis and Biotransformation**

Edited by **Bernd Nidetzky** and **Tom Desmet**

For a complete overview see the Issue and the Editorial

https://doi.org/10.1016/j.cbpa.2020.09.010

Keywords

SDR, Short-chain dehydrogenase/reductase, Decarboxylase, Epimerase, Dehydratase, Transient oxidation-reduction, Stereo-electronic effect.

Introduction

Transient oxidation–reduction is a central mechanistic principle of sugar nucleotide–modifying enzymes to achieve a variety of biosynthetically important transformations [1–5]. These transformations notably involve epimerization, decarboxylation, and dehydration (Figure 1) [3,4,6]. The enzymes catalyzing these reactions share common membership to the short-chain dehydrogenase/reductase (SDR) protein superfamily [4]. They are often referred to as 'extended SDRs' for the additional features of structure and function they involve compared with the prototypical SDR oxidoreductase [4]. They generally use a tightly bound NAD^+ or $NADP^+$ cofactor and are equipped with the basic SDR catalytic machinery (a highly conserved Asn/Ser/Tyr/Lys tetrad of residues) to facilitate oxidation–reduction [4]. The active sites of extended SDRs are often expanded by residues fulfilling deprotonation–protonation types of catalytic function [4]. Thus, the extended SDRs integrate unique reactivities (e.g., epimerization [2,7–10,11*,12,13**], β-elimination of water [14**,15*,16–18], aldol cleavage for ring opening [19*,20**], decarboxylation [20**,21,22**]) into a cycle of hydride transfer to and from the nicotinamide cofactor. Oxidation of the sugar nucleotide serves the essential role of activating the substrate for further transformations. Except in hexose nucleotide 4,6-dehydratases as discussed later, the hydride is delivered back to the same substrate carbon from which it was abstracted. The reduction is usually stereospecific, except in C2- and C4-epimerases (Figure 1, UGAepi reaction) that require nonstereospecific reduction of the corresponding 2- or 4-keto-hexose intermediate. The C2/C4-epimerases must add the feature of free rotation of the transient intermediate to enable delivery of the hydride from either face of the carbonyl group [2,5,7,10,12,13**,23,24*]. Mechanistic proposals have been worked out in considerable detail for catalytic

Figure 1

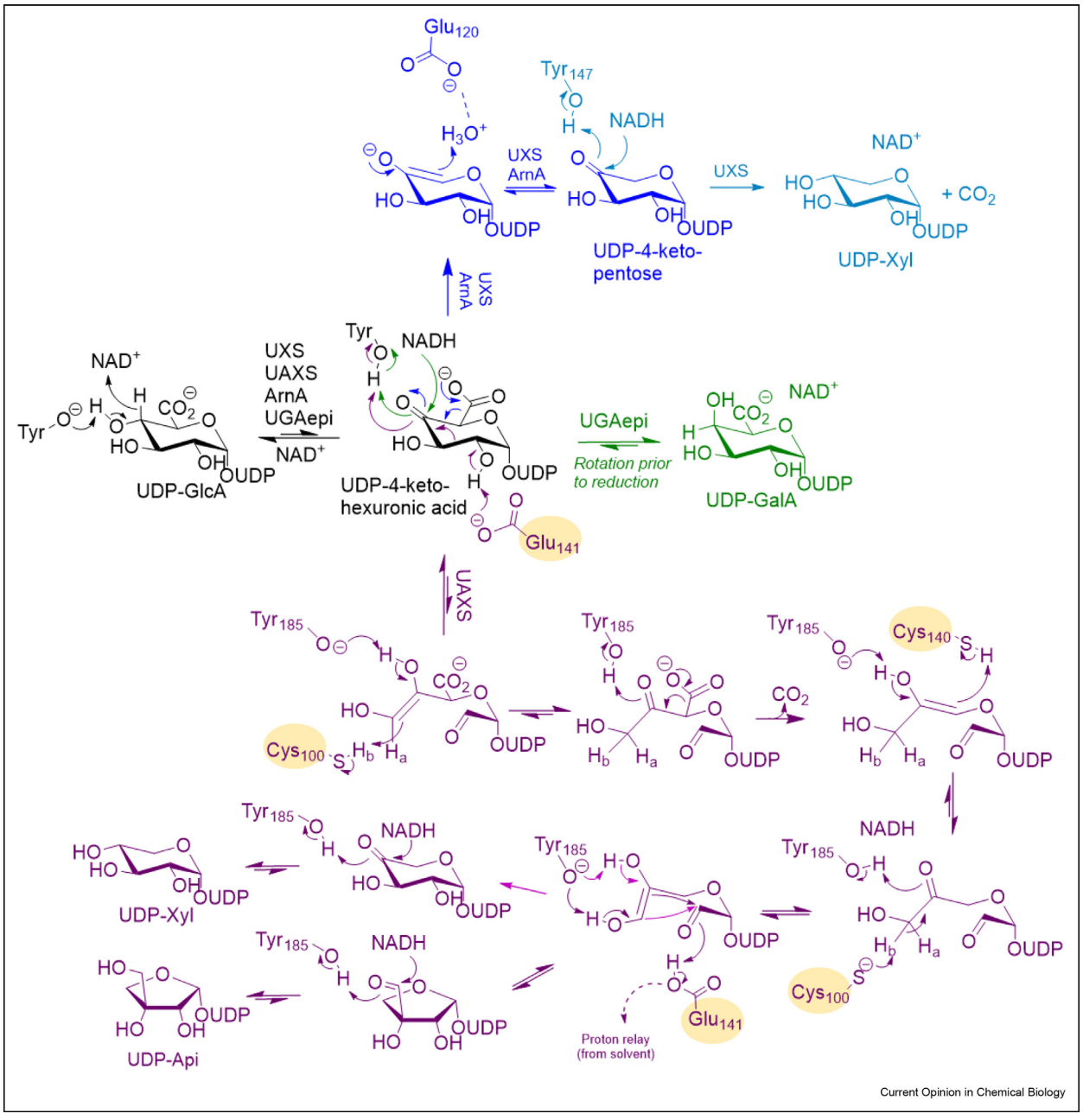

Schematic representation of the reaction mechanisms of UAXS (black/purple) [20**], UXS (black/dark blue/light blue) [22**], UGAepi (black/green) [13**], and ArnA (black/dark blue) [21]. The key residues responsible for the acid/base catalysis on the active site of UAXS are highlighted with yellow circles. UDP, uridine 5'-diphosphate; UAXS, UDP-xylose synthase; UGAepi, UDP-GlcA 4-epimerase; UXS, UDP-xylose synthase.

epimerization [2,10,13**,23,24*,25,26,27**], decarboxylation [19*,20**,21,22**], and dehydration [14**,15*,18] based on structural and biochemical studies performed on different enzymes over decades.

Despite this, the finely tuned control of reactivity and selectivity in several of these enzymes still remains a mystery. A biologically important and mechanistically striking example is represented by uridine 5'-diphosphate-glucuronic acid (UDP-GlcA), which is the common substrate for epimerase and decarboxylase types of extended SDRs (Figure 1) [19*,20**,21,22**]. The UDP-GlcA 4-epimerase (UGAepi) (EC 5.1.3.6) catalyzes the reversible interconversion of UDP-GlcA

and UDP-galacturonic acid (UDP-GalA) [7,13**,27**,28–31]. The UDP-GlcA decarboxylases (UDP-xylose synthase [UXS] EC 4.1.1.35 [22**,32]; UDP-apiose/UDP-xylose synthase [UAXS], EC 4.1.1 [19*,20**,33]; UDP-GlcA decarboxylase ArnA, EC 1.1.1.305 [21,34]) convert UDP-GlcA into different UDP-pentose products (Figure 1).

Recent studies suggest an important role for stereo-electronic control by the enzymes to steer a perfectly selective transformation of UDP-GlcA, leading to different products from the same substrate [13**,20**,22**]. The studies also indicate that stereo-electronic constraints at the active site enable the decarboxylase enzymes to achieve a unique timing of their catalytic reaction steps [20**]. The mechanistic idea of stereo-electronic control is extended to epimerases and dehydratases that deprotonate the Cα of the transient keto-hexose intermediate. In addition, the human guanosine 5'-diphosphate (GDP)-mannose 4,6-dehydratase is discussed here for the recent mechanistic insight it has provided into the elimination mechanism. Based on structure snapshots from the reaction coordinate, the enzyme was shown to use a minimal catalytic machinery comprised of just two active-site groups, exactly as predicted earlier from theoretical considerations, for the β-elimination of water from the keto-hexose species [14**].

Extended SDR enzymes for conversion of UDP-GlcA and their proposed catalytic mechanisms

The proposed reaction paths and the basic catalytic mechanisms of UGAepi, UXS, ArnA, and UAXS for the conversion of UDP-GlcA are shown in Figure 1. Each reaction is initiated by transient oxidation at substrate C4. Hydride abstraction to NAD^+ is facilitated by tyrosine (from the conserved SDR catalytic tetrad) functioning as the general base [13**,20**,21,22**,27**].

UXS and ArnA promote decarboxylation of the UDP-4-keto-hexuronic acid intermediate [21,22**]. UXS reduces the resulting UDP-4-keto-pentose stereospecifically to UDP-xylose [22**]. Contrary to UXS, ArnA lacks a tightly bound nicotinamide cofactor and must bind NAD^+ from solution [21]. Interestingly, ArnA reaction with UDP-GlcA stops at the UDP-4-keto-pentose, which is then used by a different enzyme (ArnB) in a transamination reaction with L-glutamic acid to form UDP-4-amino-4-deoxy-L-arabinose [35,36]. ArnA releases the NADH formed [21]. In UXS and ArnA, a conserved glutamic acid residue is involved in proton transfer to C5 during decarboxylation and/or fixing the substrate in place for the enzymatic conversion (Figure 2a) [21,22**]. The Glu is also conserved in hexose nucleotide 4,6-dehydratases, in which it plays the mechanistically comparable role of deprotonation-protonation at C5 [14**,15*,18,37], as discussed later.

The Glu is lacking in UGAepi (Figure 2a). Structurally, UGAepi resembles the well-characterized UDP-galactose 4-epimerase in that it provides fully formed binding pockets for NAD^+ and UDP [27**]. From the perspective of molecular structure, therefore, any repositioning of the two molecules in the course of the UGAepi catalytic cycle is highly unlikely. To perform a nonstereospecific reduction of the C4 carbonyl group, UGAepi must therefore enable free rotation of the 4-keto-hexuronic acid moiety. An interesting mechanistic challenge for UGAepi is to combine this free rotation requirement with proper protection of the chemically labile β-keto-acid intermediate against decarboxylation [13**].

The reaction of UAXS leading to UDP-apiose is unusually complex to be carried out by a single active site. The proposed mechanism involves a retro-aldol reaction for ring opening of the 4-keto-hexuronic acid intermediate [19*,20**]. The conserved Glu (Figure 2a) adopts a unique role to facilitate deprotonation of the 2-OH during aldol cleavage, as shown in Figure 1 [20**]. Two cysteine residues participate in the subsequent decarboxylation and ring-closure steps (Figure 1) [20**]. The cysteines of UAXS are not conserved in UXS and ArnA. However, cysteine residues are involved in deprotonation–protonation steps at sugar carbon in reactions of GDP-mannose 3,5-epimerase [38*] and GDP-L-fucose synthetase [39*]. Both enzymes also belong to the extended SDRs. The UAXS (from *Arabidopsis thaliana*) was shown to not catalyze ring opening on an isolated UDP-4-keto-pentopyranose intermediate [20**]. Therefore, timing of the catalytic steps, such that the ring opening occurs before the decarboxylation, appears to be essential. Ring closure establishes the ring contraction in a reversible aldol reaction. Ring closure without ring contraction appears to be effectively irreversible. Reduction leads to UDP-apiose and UDP-xylose in a ratio that seems to depend on both the enzyme and the reaction conditions used [20**].

Evidence for stereo-electronic control in reactions of UXS, UGAepi, and UAXS

As shown in Figure 1, the catalytic paths of UAXS, UXS, ArnA, and UGAepi diverge at the UDP-4-keto-hexuronic acid intermediate. To appreciate the enzymes' individual ways of handling the intermediate (a labile β-keto acid species), it is relevant to consider chemical requirements for decarboxylation in the context of a six-membered ring system. Generally, decarboxylation is stereo-electronically favored when the dihedral angle between the C=O bond and the cleaved C–C bond is ~90° (Figure 2b) [40,41]. In the

Figure 2

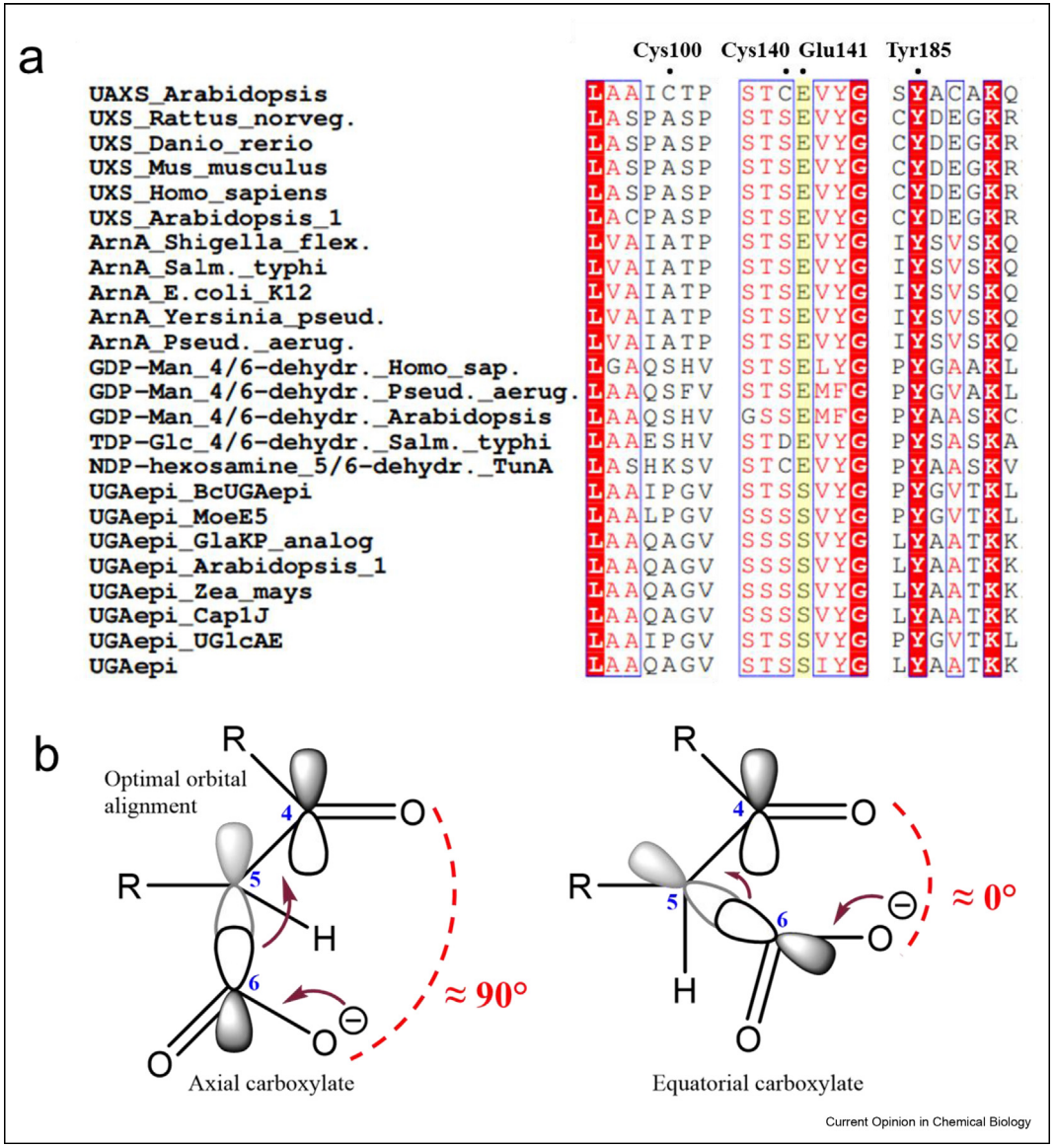

Sequence comparison of SDR epimerases, decarboxylases and dehydratases (a) and illustration of orbital alignment for decarboxylation of a β-keto acid (b). **(a)** A partial multiple sequence alignment of UAXS, UXS, ArnA, UGAepi, and NDP-sugar dehydratases. The key amino acids for the catalysis in UAXS are labeled on the top of the alignment. The conserved Glu residue in decarboxylases and dehydratases (Ser in UGAepis) is highlighted in yellow. **(b)** Orbital alignment in decarboxylation of a β-keto acid with the axial (left) and equatorial (right) carboxylate moiety. The C5 p-orbital on the incipient 4,5-enolate is shown in light gray. GDP-Man, guanosine 5'-diphosphate-mannose; TDP-Glc, thymidine 5'-diphosphate glucose; UAXS, UDP-xylose synthase; UGAepi, UDP-GlcA 4-epimerase; UXS, UDP-xylose synthase.

UDP-4-keto-hexuronic acid intermediate, a dihedral of ~90° requires the carboxylate group to be positioned axially. Chemical studies show that optimal orbital alignment for decarboxylation involves a continuous overlap, via hyperconjugation and resonance, from the breaking C–C bond and the π-orbital of the carbonyl (C4=O) group [41–43]. In the stereo-electronically optimal case for the enzymatic decarboxylation (axial carboxylate), the breaking C5–C6 bond is roughly orthogonal to the plane of the C5–C4=O system, allowing for productive σ–π delocalization [43] to enable good overlap of the π-orbital system of the carbonyl carbon (C4) with the developing C5 p-orbital in the incipient 4,5-enolate [41,43] (Figure 2b). To bring the carboxylate into an axial position at the enzyme's active site, a binding energy–driven distortion from the pyranose chair conformation may be necessary. The relaxed chair conformation of the 4-keto-hexuronic acid features an equatorial carboxylate with a dihedral angle of ~0°. The equatorial carboxylate thus provides stereo-electronic constraints nonoptimal for decarboxylation. For an enzymatic path to exclude (UGAepi), or to delay (UAXS), the decarboxylation, therefore, a stereo-electronic rational to maintain an equatorial carboxylate is thus provided. The mechanistic idea of differential stereo-electronic control in epimerase and decarboxylase reactions of UDP-GlcA is supported by a comparison of UXS and UGAepi. Binding of UDP-GlcA by UAXS is also consistent with the overall stereo-electronic argument. The importance of proper orbital alignment for promoting or preventing decarboxylation has been recognized over decades in studies of pyridoxal 5'-phosphate (PLP)-dependent enzymes, where the enzyme applies stereo-electronic constraints to 'choose' between decarboxylation and transamination/racemization [42,44–46].

Figure 3

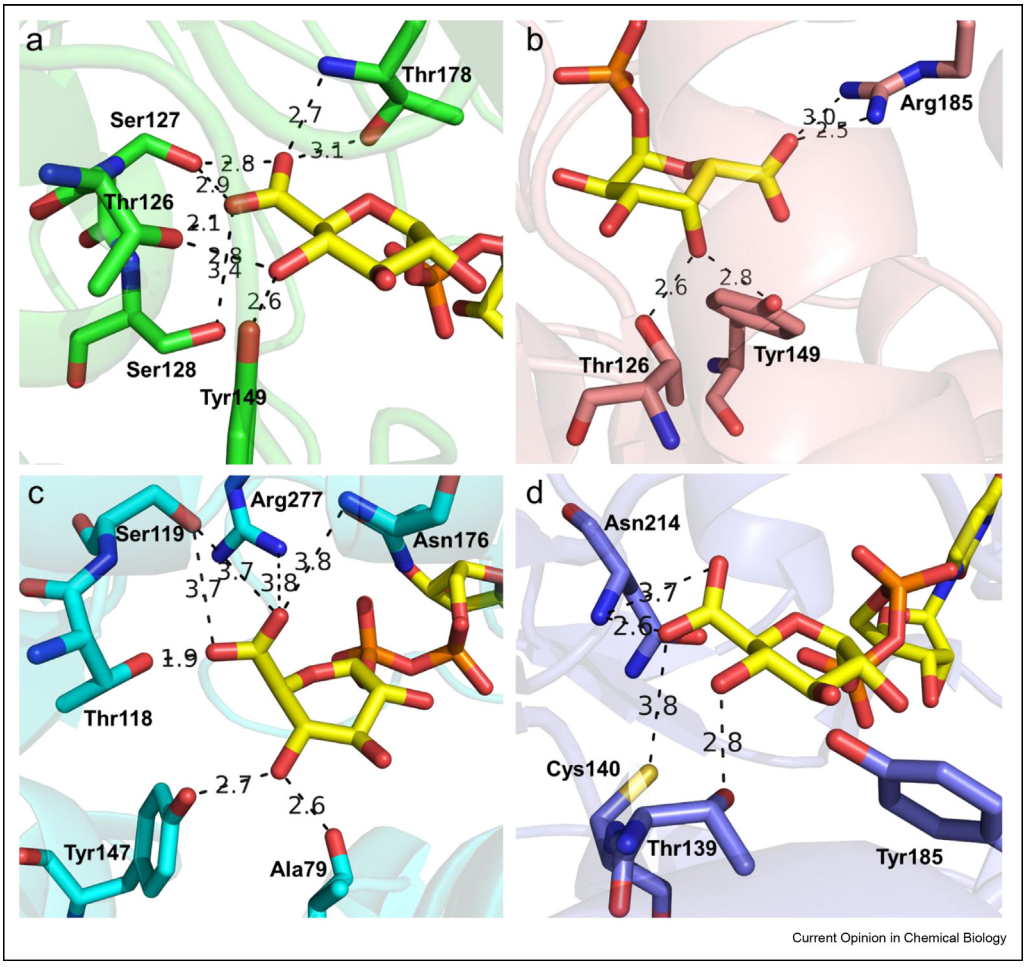

Active site close-ups of BcUGAepi **(a,b)**, UXS **(c)**, and UAXS **(d)** showing the interactions with the carboxylate and C4–OH of the substrate (yellow carbons). **(a)** The substrate complex of BcUGAepi (green; PDB: 6Z73, [27**]) with UDP-GlcA. The carboxylate moiety is positioned equatorially. **(b)** The product complex of BcUGAepi (salmon; PDB: 6Z75, [27**]) with UDP-GalA showing the equatorial carboxylate. Structure of UXS (cyan; PDB: 2B69, [22**]) highlighting the perfectly axial carboxylate moiety of UDP-GlcA. **(c)** The substrate complex of UAXS (blue; PDB: 6H0P, [20**]) showing the equatorial carboxylate of UDP-GlcA.

Structures of UGAepi bound with UDP-GlcA (Figure 3a) and UDP-GalA (Figure 3b) show the pyranose ring in an undistorted $^4C_1$ conformation, which places the carboxylate group equatorially [27**]. In each structure, the carboxylate is accommodated within a tight network of hydrogen bonds. The reactive 4-OH of the substrate/product is well aligned with the catalytic residues of the enzyme. Threonine from the SDR catalytic triad orients the 4-OH for proton abstraction by tyrosine. Interestingly, the threonine is also close to the substrate/product carboxylate. Besides establishing stereo-electronic conditions to disfavor decarboxylation, binding of the carboxylate group could arguably contribute to precise positioning of the substrate for catalysis. Binding constraints from the active site pose a conundrum for UGAepi given the requirement for free rotation of the 4-keto-hexuronic acid intermediate for epimerization. Computational analysis will be important to elucidate dynamic features of the catalytic reaction. The conformational rearrangements associated with the rotation have now been captured at high resolution in the crystal [27**].

For UXS, the conformation of the Michaelis complex was derived from a high-resolution crystal structure of the human enzyme bound with NAD^+ and UDP. The UDP-GlcA was modeled into the active site [22**]. Molecular dynamics computational studies revealed that to achieve a plausible positioning of GlcA for catalysis the pyranose $^4C_1$ chair had to be distorted. A $B_{O,3}$ boat conformation, placing the carboxylate in an almost perfect axial position 'ready for decarboxylation', was found to yield a seemingly proper alignment between the reactive groups on the substrate (UDP-GlcA), cofactor (NAD^+), and the catalytic groups on the enzyme (Figure 3c) [22**]. UXS provides fewer interactions with the substrate carboxylate than UGAepi, and binding of the carboxylate lacks the direct connection to the immediate catalytic machinery. The crystal structure of ArnA bound with UDP-GlcA shows an undistorted chair conformation for the pyranose ring with the carboxylate in the equatorial position. However, the substrate is not positioned for catalytic oxidation at C4 to occur via the canonical SDR mechanism, and, therefore, a nonproductive enzyme–substrate complex appears to have been captured in the ArnA crystal [21].

The special case of UAXS: precise timing of decarboxylation in multistep SDR catalysis

Similar as in UXS, molecular dynamics simulations had to be done on the experimental enzyme crystal structure (the C100A variant of *A. thaliana* UAXS bound with NADH and UDP-GlcA) to identify the plausible conformation of the Michaelis complex [20**]. The substrate-bound conformation of the enzyme's active site is unusually flexible, with the pyranose ring pucker changing substantially along simulated trajectories. The enzyme complex conformations featuring a plausible positioning of UDP-GlcA for the initial catalytic step (oxidation at C4) all have the carboxylate group in a closely equatorial position, as shown in Figure 3d. This supports the particular timing of UAXS catalytic steps that delays the decarboxylation of the β-keto-acid until after the ring opening between C2 and C3 has happened. The ring-opened intermediate can then position the carboxylate moiety for suitable orbital alignment to meet the stereo-electronic requirements for efficient decarboxylation [20**].

Stereo-electronic considerations extended to other epimerases and dehydratases

In pyranose ring systems, the α-proton of a ketone is more easily abstracted (i.e., becomes more acidic) when it is positioned axially [38*,47]. Concerning the orbital alignment optimal for deprotonation, effectively the same considerations (σ–π delocalization) apply as for decarboxylation [41,43,47]. Structural and mechanistic studies of hexose nucleotide 4,6-dehydratases (e.g., thymidine 5'-diphosphate (dTDP)-glucose 4,6-dehydratase; cytidine 5'-diphosphate (CDP)-glucose 4,6-dehydratase; GDP-mannose 4,6-dehydratases) [14**,37,48–54] and epimerases acting on the α-carbon(s) (e.g., GDP-mannose 3,5-epimerase [38*]; GDP-L-fucose synthetase [39*,55]) suggest that each enzyme applies stereo-electronic control. Changes in sugar ring pucker can be important to meet the stereo-electronic requirements for efficient deprotonation/protonation, as shown for GDP-mannose 3,5-epimerase [38*,39*].

Recent study of the human GDP-mannose 4,6-dehydratase has rekindled mechanistic considerations of Gerlt and Gassman [56*] for the enzymatic β-elimination of a ketone [14**,56*]. Their suggestion was that the lowest energy pathway for the reaction is a stepwise general acid/general base–catalyzed formation of an enol intermediate followed by 1,4-(E2-like)-elimination from the enol (not an E1cB mechanism via an enolate) [56*]. They also considered that, given suitable geometry of the enzyme–substrate complex, as shown in Figure 4a, the conjugate acid of the base catalyzing the enol formation could also catalyze expulsion of the β-substituent [56*]. The proposed mechanism implies a *syn* stereochemical course for the β-elimination reaction and suggests two as the minimal number of functional groups required for efficient catalysis [56*]. However, precatalytic and postcatalytic complex structures of the human GDP-mannose 4,6-dehydratase (hGMD) suggest that the enzyme represents a perfect realization of the chemical principle in its most parsimonious form [14**]. The proposed enzymatic mechanism is shown in Figure 4b. Concerted catalysis by Tyr179 and Glu157 is involved in the formation of the enol intermediate. Molecular dynamics simulations revealed the essential side chain

Figure 4

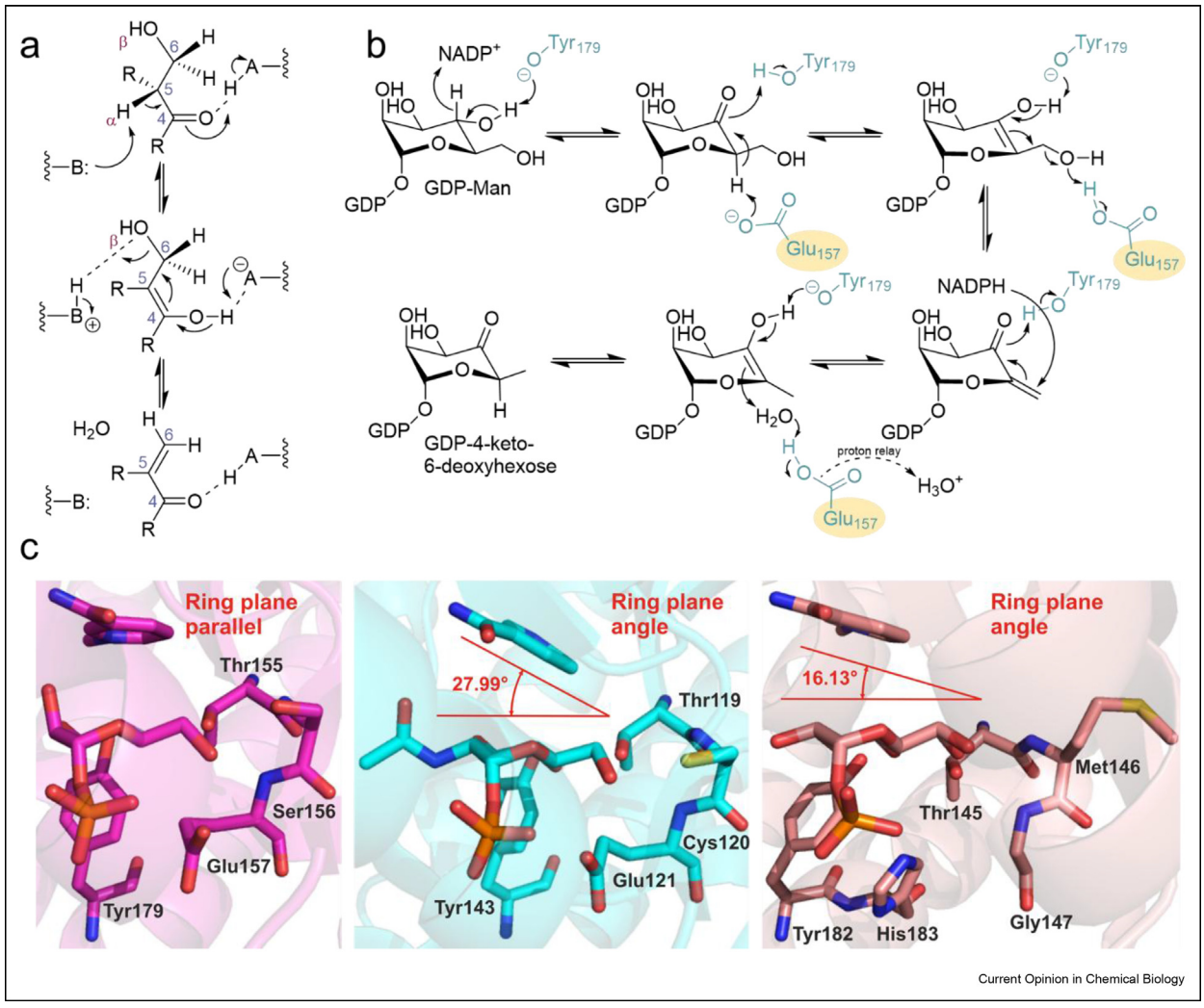

The proposed catalytic mechanism of dehydration by hGMD (a, b) and active site close ups of hGMD, TunA and SQD1 (c). **(a)** The **stepwise** mechanism **of β-el**imination of water from a ketone as implemented into the hGMD active site. **(b)** The mechanism of guanosine 5'-diphosphate-mannose (GDP-Man) 4,6-dehydration catalyzed by hGMD [14**]. **(c)** Relative positions and angles of substrates and cofactors in the active sites of hGMD (purple, PDB: 6GPJ, [14**]), TunA (cyan, PDB: 3VPS, [15*]), and SQD1 (salmon, PDB: 1QRR, [16]).

conformational flexibility for Glu157, so that it could function as a catalytic base during the enol formation and, in conjugate acid form, as a catalytic acid during the expulsion of water [14**]. Further reaction to product proceeds in two steps, representing in opposite order the reversal of the previous catalytic steps of oxidation and enolization [14**]. In the UDP-GlcNAc 5,6-dehydratase (TunA) [15*] and in the UDP-sulfoquinose synthase (SQD1, Agl3) [16–18], the initial oxidation and β-elimination are catalyzed analogously as described for the 4,6-dehydratases, whereas SQDs utilize His instead of Asp as the general acid/base catalyst. However, reduction of the C4-carbonyl, instead of the 5,6-ene, results in the formation of a 5,6-ene product or reaction intermediate in case of TunA and SQDs, respectively [15*–18]. The regioselectivity of the reduction is controlled by a fine-tuned alignment of nicotinamide ring of the NAD^+ cofactor relative to the sugar ring plane. In 4,6-dehydratases a parallel alignment is observed, allowing hydride abstraction from C4 and re-donation to C6. In contrast, a nonparallel alignment is observed in TunA and SQD1 with an angle of around 15–30° to each other, favoring re-donation of the hydride to C4 (Figure 4c) [14**,15*].

Conclusion

Constraining substrates into optimal conformations is an essential aspect of enzymatic catalysis [57]. Enzymes promote proper orientation of the orbitals to facilitate the desired biochemical transformation [42,57–59].

The contribution of stereo-electronic effects into enzyme-catalyzed reactions has been appreciated for decades, especially in context where enzymes apply stereo-electronic control to either allow or exclude certain reaction pathways [42,57,58,60,61]. Recent studies on SDR decarboxylases (UAXS, UXS, ArnA) [19*,20**,21,22**] and epimerases (UGAepi) [13**,27**] demonstrate how structurally closely related enzymes can utilize effectively the same substrate (UDP-GlcA) to catalyze different reaction pathways (decarboxylation, epimerization, aldol cleavage for ring opening) assisted by stereo-electronic control. This fascinating concept can be expanded to NDP-sugar dehydratases (hGMD, TunA, SQD) [14**,15*,18] from the SDR superfamily, where stereo-electronic constraints contribute to the regioselectivity of the reaction. In addition, the studies from the last few years highlight how essentially the same active site of the SDR epimerases, decarboxylases, and dehydratases is fine-tuned to perform different catalytic pathways. Realizing the importance of proper orbital alignment in (bio)chemical reactions is crucial for mechanistic enzymology and will be helpful in understanding the enzymatic mechanisms in future.

Declaration of competing interest

Nothing declared.

Acknowledgement

Financial support through the EpiSwitch and DeoxyBioCat projects, both jointly funded by the Austrian Science Fund (FWF; projects I 3247 and I 4516-B, respectively; B.N.) and the Fund for Scientific Research Flanders, Belgium (FWO-Vlaanderen, grant n° G0F3417N and G0A7520N, respectively; T.D.), are gratefully acknowledged.

References

Papers of particular interest, published within the period of review, have been highlighted as:

* of special interest
** of outstanding interest

1. Field RA, Naismith JH: **Structural and mechanistic basis of bacterial sugar nucleotide-modifying enzymes**. *Biochemistry* 2003, **42**:7637–7647.

2. Allard STM, Giraud M-F, Naismith JH: **Epimerases: structure, function and mechanism**. *Cell Mol Life Sci* 2001, **58**: 1650–1665.

3. Thibodeaux CJ, Melançon CE, Liu HW: **Unusual sugar biosynthesis and natural product glycodiversification**. *Nature* 2007, **446**:1008–1016.

4. Kavanagh KL, Jörnvall H, Persson B, Oppermann U: **Medium- and short-chain dehydrogenase/reductase gene and protein families: the SDR superfamily: functional and structural diversity within a family of metabolic and regulatory enzymes**. *Cell Mol Life Sci* 2008, **65**:3895–3906.

5. Samuel J, Tanner ME: **Mechanistic aspects of enzymatic carbohydrate epimerization**. *Nat Prod Rep* 2002, **19**:261–277.

6. Reiter W-D: **Biochemical genetics of nucleotide sugar interconversion reactions**. *Curr Opin Plant Biol* 2008, **11**:236–243.

7. Sun H, Ko TP, Liu W, Liu W, Zheng Y, Chen CC, Guo RT: **Structure of an antibiotic-synthesizing UDP-glucuronate 4-epimerase MoeE5 in complex with substrate**. *Biochem Biophys Res Commun* 2020, **521**:31–36.

8. Van Overtveldt S, Gevaert O, Cherlet M, Beerens K, Desmet T: **Converting galactose into the rare sugar talose with cellobiose 2-epimerase as biocatalyst**. *Molecules* 2018, **23**.

9. Gevaert O, Van Overtveldt S, Beerens K, Desmet T: **Characterization of the first bacterial and thermostable GDP-mannose 3,5-epimerase**. *Int J Mol Sci* 2019, **20**.

10. Van Overtveldt S, Verhaeghe T, Joosten HJ, van den Bergh T, Beerens K, Desmet T: **A structural classification of carbohydrate epimerases: from mechanistic insights to practical applications**. *Biotechnol Adv* 2015, **33**:1814–1828.

11. * Nam YW, Nishimoto M, Arakawa T, Kitaoka M, Fushinobu S: **Structural basis for broad substrate specificity of UDP-glucose 4-epimerase in the human milk oligosaccharide catabolic pathway of *Bifidobacterium longum***. *Sci Rep* 2019, **9**:11081.
This article provides an excellent discussion and overview for the substrate specificity determinants in UDP-glucose 4-epimerases.

12. Hallis TM, Zhao Z, Liu HW: **New insights into the mechanism of CDP-D-tyvelose 2-epimerase: an enzyme-catalyzing epimerization at an unactivated stereocenter**. *J Am Chem Soc* 2000, **122**:10493–10503.

13. ** Borg AJE, Dennig A, Weber H, Nidetzky B: **Mechanistic characterization of UDP-glucuronic acid 4-epimerase**. *FEBS J* 2020, https://doi.org/10.1111/febs.15478.
This article discusses and explains the impact of stereo-electronic control on the UDP-glucuronic acid 4-epimerase reaction.

14. ** Pfeiffer M, Johansson C, Krojer T, Kavanagh KL, Oppermann U, Nidetzky B: **A parsimonious mechanism of sugar dehydration by human GDP-mannose-4,6-dehydratase**. *ACS Catal* 2019, **9**: 2962–2968.
An important research paper deciphering the reaction mechanism of GDP-mannose 4,6-dehydration catalyzed by the minimal catalytic machinery of GDP-mannose 4,6-dehydratase.

15. * Wyszynski FJ, Lee SS, Yabe T, Wang H, Gomez-Escribano JP, Bibb MJ, Lee SJ, Davies GJ, Davis BG: **Biosynthesis of the tunicamycin antibiotics proceeds via unique exo-glycal intermediates**. *Nat Chem* 2012, **4**:539–546.
The authors describe the crystal structure and decipher the reaction mechanism of UDP-GlcNAc 5,6-dehydratase while discovering the determinants for the regioselectivity of the final reduction step.

16. Mulichak AM, Theisen MJ, Essigmann B, Benning C, Garavito RM: **Crystal structure of SQD1, an enzyme involved in the biosynthesis of the plant sulfolipid headgroup donor UDP-sulfoquinovose**. *Proc Natl Acad Sci U S A* 1999, **96**: 13097–13102.

17. Sanda S, Leustek T, Theisen MJ, Garavito RM, Benning C: **Recombinant *Arabidopsis* SQD1 converts UDP-glucose and sulfite to the sulfolipid head group precursor UDP-sulfoquinovose in vitro**. *J Biol Chem* 2001, **276**:3941–3946.

18. Zolghadr B, Gasselhuber B, Windwarder M, Pabst M, Kracher D, Kerndl M, Zayni S, Hofinger-Horvath A, Ludwig R, Haltrich D, *et al.*: **UDP-sulfoquinovose formation by *Sulfolobus acidocaldarius***. *Extremophiles* 2015, **19**:451–467.

19. * Eixelsberger T, Horvat D, Gutmann A, Weber H, Nidetzky B: **Isotope probing of the UDP-apiose/UDP-xylose synthase reaction: evidence of a mechanism via a coupled oxidation and aldol cleavage**. *Angew Chem Int Ed* 2017, **56**:2503–2507.
This article discusses the first direct evidence for the pyranoside-to-furanoside ring contraction in the catalytic pathway of UDP-apiose/UDP-xylose synthase.

20. ** Savino S, Borg AJE, Dennig A, Pfeiffer M, De Giorgi F, Weber H, Dubey KD, Rovira C, Mattevi A, Nidetzky B: **Deciphering the enzymatic mechanism of sugar ring contraction in UDP-apiose biosynthesis**. *Nat Catal* 2019, **2**:1115–1123.
This work reveals the detailed enzymatic mechanism of UDP-apiose/UDP-xylose synthase and illustrates how the timing of the catalytic steps is supported by stereo-electronic control applied by the enzyme.

21. Gatzeva-Topalova PZ, May AP, Sousa MC: **Structure and mechanism of ArnA: conformational change implies ordered**

dehydrogenase mechanism in key enzyme for polymyxin resistance. *Structure* 2005, **13**:929–942.

22. ** Eixelsberger T, Sykora S, Egger S, Brunsteiner M, Kavanagh KL, Oppermann U, Brecker L, Nidetzky B: **Structure and mechanism of human UDP-xylose synthase: evidence for a promoting role of sugar ring distortion in a three-step catalytic conversion of UDP-glucuronic acid**. *J Biol Chem* 2012, **287**: 31349–31358.
Here the authors describe how UDP-xylose synthase utilizes stereo-electronic control, i.e. promotes a change in its substrate's ring pucker, to facilitate the catalyzed reaction.

23. Beerens K, Soetaert W, Desmet T: **UDP-hexose 4-epimerases: a view on structure, mechanism and substrate specificity**. *Carbohydr Res* 2015, **414**:8–14.

24. * Frey PA, Hegeman AD: **Chemical and stereochemical actions of UDP–galactose 4-epimerase**. *Acc Chem Res* 2013, **46**: 1417–1426.
This review gives an excellent overview of the catalytic mechanism of UDP-galactose 4-epimerase.

25. Ishiyama N, Creuzenet C, Lam JS, Berghuis AM: **Crystal structure of WbpP, a genuine UDP-N-acetylglucosamine 4-epimerase from *Pseudomonas aeruginosa*: substrate specificity in UDP-hexose 4-epimerases**. *J Biol Chem* 2004, **279**: 22635–22642.

26. Berger E, Arabshahi A, Wei Y, Schilling JF, Frey PA: **Acid - base catalysis by UDP-galactose 4-epimerase: correlations of kinetically measured acid dissociation constants with thermodynamic values for tyrosine 149**. *Biochemistry* 2001, **40**: 6699–6705.

27. ** Iacovino LG, Savino S, Borg AJE, Binda C, Nidetzky B, Mattevi A: **Crystallographic snapshots of UDP-glucuronic acid 4-epimerase ligand binding, rotation and reduction**. *J Biol Chem* 2020 [Manucript accepted for publication].
Here the authors have captured several high resolution crystal structures of UDP-glucuronic acid 4-epimerase, including a unique structure where the substrate- and product-bound enzymes coexist within the same crystal.

28. Feingold DS, Neufeld EF, Hassid WZ: **The 4-epimerization and decarboxylation of uridine diphosphate D-glucuronic acid by extracts from *Phaseolus aureus* seedlings**. *J Biol Chem* 1960, **235**:910–913.

29. Munoz R, Lopez R, de Frutos M, Garcia E: **First molecular characterization of a uridine diphosphate galacturonate 4-epimerase: an enzyme required for capsular biosynthesis in Streptococcus pneumoniae type 1**. *Mol Microbiol* 1999, **31**: 703–713.

30. Broach B, Gu X, Bar-Peled M: **Biosynthesis of UDP-glucuronic acid and UDP-galacturonic acid in *Bacillus cereus* subsp. cytotoxis NVH 391-98**. *FEBS J* 2012, **279**:100–112.

31. Gu X, Bar-Peled M: **The biosynthesis of UDP-galacturonic acid in plants. Functional cloning and characterization of Arabidopsis UDP-d-glucuronic acid 4-epimerase**. *Plant Physiol* 2004, **136**:4256–4264.

32. Moriarity JL, Joseph Hurt K, Resnick AC, Storm PB, Laroy W, Schnaar RL, Snyder SH: **UDP-glucuronate decarboxylase, a key enzyme in proteoglycan synthesis. Cloning, characterization, and localization**. *J Biol Chem* 2002, **277**:16968–16975.

33. Sandermann H, Tisue GT, Grisebach H: **Biosynthesis of d-apiose IV. Formation of UDP-apiose from UDP- d-glucuronic acid in cell-free extracts of parsley (*Apium petroselinum L.*) and *Lemna minor***. *Biochim Biophys Acta Gen Subj* 1968, **165**: 550–552.

34. Gatzeva-Topalova PZ, May AP, Sousa MC: **Crystal structure of *Escherichia coli* ArnA (PmrI) decarboxylase domain. A key enzyme for lipid A modification with 4-amino-4-deoxy- l -arabinose and polymyxin resistance**. *Biochemistry* 2004, **43**: 13370–13379.

35. Breazeale SD, Ribeiro AA, Raetz CRH: **Origin of lipid a species modified with 4-amino-4-deoxy-l-arabinose in polymyxin-resistant mutants of *Escherichia coli*: an aminotransferase (ArnB) that generates UDP-4-amino-4-deoxy-L-arabinose**. *J Biol Chem* 2003, **278**:24731–24739.

36. Noland BW, Newman JM, Hendle J, Badger J, Christopher JA, Tresser J, Buchanan MD, Wright TA, Rutter ME, Sanderson WE, *et al.*: **Structural studies of *Salmonella typhimurium* ArnB (PmrH) aminotransferase: a 4-amino-4-deoxy-l-arabinose lipopolysaccharide-modifying enzyme**. *Structure* 2002, **10**: 1569–1580.

37. Allard STM, Beis K, Giraud MF, Hegeman AD, Gross JW, Wilmouth RC, Whitfield C, Graninger M, Messner P, Allen AG, *et al.*: **Toward a structural understanding of the dehydratase mechanism**. *Structure* 2002, **10**:81–92.

38. * Major LL, Wolucka BA, Naismith JH: **Structure and function of GDP-mannose-3′,5′-epimerase: an enzyme which performs three chemical reactions at the same active site**. *J Am Chem Soc* 2005, **127**:18309–18320.
This work illustrates how GDP-mannose 3,5-epimerase applies stereo-electronic control by the means of ring flip and pucker change to direct the regioselectivity of the catalyzed reaction.

39. * Lau STB, Tanner ME: **Mechanism and active site residues of GDP-fucose synthase**. *J Am Chem Soc* 2008, **130**: 17593–17602.
Here the authors elucidate the unusually complex sequence of two epimerizations and a reduction catalyzed by a single active site of GDP-fucose synthase.

40. Pollack RM: **Stereoelectronic control in the reactions of ketones and their enol(ate)s**. *Tetrahedron* 1989, **45**:4913–4938.

41. Kayser RH, Brault M, Pollack RM, Bantia S, Sadoff SF: **Kinetics of decarboxylation of the two epimers of 5-ieri-butyl-l-methyl-2-oxocyclohexanecarboxylic acid: lack of stereoelectronic control in β-keto acid decarboxylation**. *J Org Chem* 1983, **48**: 4497–4502.

42. Toney MD: **Controlling reaction specificity in pyridoxal phosphate enzymes**. *Biochim Biophys Acta Protein Proteonomics* 2011, **1814**:1407–1418.

43. Behnam SM, Behnam SE, Ando K, Green NS, Houk KN: **Stereoelectronic, torsional, and steric effects on rates of enolization of ketones**. *J Org Chem* 2000, **65**:8970–8978.

44. Dunathan HC: **Conformation and reaction specificity in pyridoxal phosphate enzymes**. *Proc Natl Acad Sci U S A* 1966, **55**: 712–716.

45. Fogle EJ, Liu W, Woon S-T, Keller JW, Toney MD: **Role of Q52 in catalysis of decarboxylation and transamination in dialkylglycine decarboxylase**. *Biochemistry* 2005, **44**:16392–16404.

46. Walsh CT: **Biologically generated carbon dioxide: nature's versatile chemical strategies for carboxy lyases**. *Nat Prod Rep* 2020, **37**:100–135.

47. Corey EJ: **The stereochemistry of α-haloketones. V. Prediction of the stereochemistry of α-brominated ketosteroids**. *J Am Chem Soc* 1954, **76**:175–179.

48. Koropatkin NM, Holden HM: **Structure of CDP-D-glucose 4,6-dehydratase from Salmonella typhi complexed with CDP-D-xylose**. *Acta Crystallogr Sect D Biol Crystallogr* 2005, **61**: 365–373.

49. Beis K, Allard STM, Hegeman AD, Murshudov G, Philp D, Naismith JH: **The structure of NADH in the enzyme dTDP-D-glucose dehydratase (RmlB)**. *J Am Chem Soc* 2003, **125**: 11872–11878.

50. Vogan EM, Bellamacina C, He X, Liu HW, Ringe D, Petsko GA: **Crystal structure at 1.8 Å resolution of CDP-D-glucose 4,6-dehydratase from Yersinia pseudotuberculosis**. *Biochemistry* 2004, **43**:3057–3067.

51. Mulichak AM, Bonin CP, Reiter WD, Garavito RM: **Structure of the MUR1 GDP-mannose 4,6-dehydratase from Arabidopsis thaliana: implications for ligand binding and specificity**. *Biochemistry* 2002, **41**:15578–15589.

52. Ferek JD, Thoden JB, Holden HM: **Biochemical analysis of a sugar 4,6-dehydratase from Acanthamoeba polyphaga Mimivirus**. *Protein Sci* 2020, **29**:1148–1159.

53. Riegert AS, Thoden JB, Schoenhofen IC, Watson DC, Young NM, Tipton PA, Holden HM: **Structural and biochemical investigation of PglF from Campylobacter jejuni reveals a new**

mechanism for a member of the short chain dehydrogenase/reductase superfamily. *Biochemistry* 2017, **56**:6030–6040.

54. Allard STM, Cleland WW, Holden HM: **High resolution X-ray structure of dTDP-glucose 4,6-dehydratase from streptomyces venezuelae**. *J Biol Chem* 2004, **279**:2211–2220.

55. Menon S, Stahl M, Kumar R, Xu GY, Sullivan F: **Stereochemical course and steady state mechanism of the reaction catalyzed by the GDP-fucose synthetase from Escherichia coli**. *J Biol Chem* 1999, **274**:26743–26750.

56. * Gerlt JA, Gassman PG: **Understanding enzyme-catalyzed proton abstraction from carbon acids: details of stepwise mechanisms for β-elimination reactions**. *J Am Chem Soc* 1992, **114**:5928–5934.
This article deciphers the pre-requisites and detailed mechanism of enzyme-catalyzed β-elimination reactions.

57. Gorenstein DG: **Stereoelectronic effects in biomolecules**. *Chem Rev* 1987, **87**:1047–1077.

58. Kirby AJ: *Stereoelectronic effects on reactivity: the kinetic anomeric effect*. 1983:78–135.

59. Mesecar AD, Stoddard BL, Koshland DE: **Orbital steering in the catalytic power of enzymes: small structural changes with large catalytic consequences**. *Science (80-)* 1997, **277**:202–206.

60. Fortner KC, Shair MD: **Stereoelectronic effects dictate mechanistic dichotomy between Cu(II)-catalyzed and enzyme-catalyzed reactions of malonic acid half thioesters**. *J Am Chem Soc* 2007, **129**:1032–1033.

61. Gorenstein DG, Findlay JB, Luxon BA, Kar D: **Stereoelectronic control in carbon-oxygen and phosphorus-oxygen bond breaking processes. Ab initio calculations and speculations on the mechanism of action of ribonuclease A, staphylococcal nuclease, and lysozyme**. *J Am Chem Soc* 1977, **99**:3473–3479.